Progress In Electromagnetics Research, PIER 87, 279–296, 2008

APPLICATION OF TRM IN THE UWB THROUGH WALL RADAR

W. Zheng, Z. Zhao, and Z. Nie

School of Electronic Engineering
University of Electronic Science and Technology of China
Chengdu, Sichuan 610054, China

Abstract—Time Reversal Mirror (TRM) technique, in the virtue of its high resolution in the heterogeneous media, has been widely applied in the area of acoustics and electromagnetics. In this paper, the technique is developed to imaging targets in the contest of ultra-wideband (UWB) through wall radar (TWR) through numerical simulation. We firstly consider the technique to image targets behind a single-layered wall and then extend to the multi-layered wall. The simulation results have reported the imaging capability of the algorithm and its powerful use for TWR imaging. For concerning the image stability, we investigate the TRM images for the case in which there is a mismatch between the walls associated with the forward and inverse phases of time reversal. The back projection imaging algorithm is compared here at the same time for a contrast of the imaging quality. Finally, some conclusions are drawn.

1. INTRODUCTION

Recent years, practical interests arising from rescue missions, behind-the-wall target detection, surveillance and reconnaissance et al., claim for high capability of imaging in complicated environments. Through Wall Radar (TWR) attracts great attentions in these areas. The imaging requires the ability to detect targets through materials such as concrete, bricks, dry wall, and plywood. Relatively high-density materials like concrete and bricks can result in considerable attenuation of electromagnetic waves and cause the multi-path propagation of the signal. This increases the requirements for both radar power and signal processing. With recent advances in both algorithms and component technologies, through wall imaging is emerging as

an affordable technology supporting a variety of civil and military applications [1–3].

Conventional narrow-band systems, such as Doppler radar and interferometric radar, are no longer applicable here due to their insufficient down-range resolution. In contrast, UWB radar, which has been investigated for TWR imaging in recent years, is the most promising candidate due to its high resolution (theoretically sub-centimeter resolution) and high power efficiency (because of low transmit duty cycle). Several papers [4–7] have reported the applications of UWB technique to TWR. And some UWB TWR systems have been built [8–11].

For the TWR imaging, several effective imaging algorithms (e.g., [12–16]) have been proposed and discussed. [12] developed an 2D contrast source inversion (CSI)-based imaging technique in a layered medium to model the effects of the building walls. [13] introduced the back projection imaging algorithm to the stepped-frequency TWR. In [16], based on higher order statistics, the author presented an autofocusing technique to correct for errors under unknown walls. However, in the heterogeneous and highly scattering environment, although the back-scattered signal level may be sufficiently above the mise level, signal between target and radar may experiences many reflections and diffractions. Therefore, many imaging methods may need complex process to minify multipath effects, i.e., to compensate the effects of the walls, such as refraction, attenuation, et al.. Considering the features of the complex environment in TWR imaging, this communication induces the time reversal mirror (TRM) technique to TWR. The TRM has been demonstrated both theoretically and experimentally in an extensive set of ultrasonic and acoustic measurements [17–23], as well as in recent electromagnetic studies [24–31]. It can provide a high-resolution image in both spatial and temporal. In this communication, FDTD algorithm is employed to simulate the electromagnetic wave propagation in the UWB through wall environment. A number of tests with numerical data to validate the 2-D electromagnetic TRM imaging in the contest of UWB through wall imaging were investigated and discussed. We firstly consider the technique to image targets behind a single-layered wall and then extend to multi-layered wall. The simulation results show the imaging capability of the algorithm and its powerful use for TWR imaging. The imaging results are much better than that of using the back projection imaging algorithm. For concerning the image stability, we also investigate the TRM images for the case in which there is a mismatch between the walls associated with the forward and inverse phases of time reversal. The conclusions here are consistent with

previous studies in [28, 32].

This paper is organized as follows: we briefly provide in Section 2 the main principles of TRM technique. It is introduced to through wall imaging in Section 3. We investigate its imaging capacities under the conditions of single- and multi- layered wall. The imaging results for using TRM are compared with that of using the back projection imaging algorithm. Some useful conclusions are drawn in the last section.

2. TIME REVERSAL MIRROR (TRM) TECHNIQUE

TRM is a technique which is based on the principle of reciprocity. Its basic principle is depicted in Fig. 1. Assume a source emits radiation that propagates through a complex media with the time-domain fields measured by an array of receivers. The recorded signals are time reversed in the time domain (or phase conjugating in the frequency

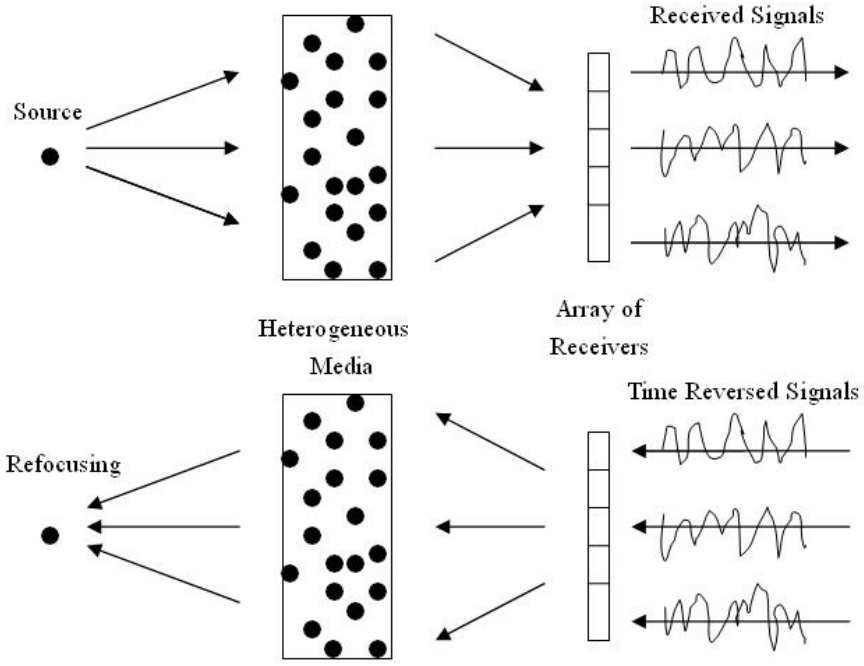

Figure 1. Time reversal basic procedure. Top: forward propagation of signals and measurements in time. Bottom: time reversing of received signals and back propagation into the media.

domain), re-emitted from their respective reception points. Due to the principle of reciprocity, all of the energy arrives at the original source in unison, approximately recreating the original excitation. The transmitter-receiver array has been termed as time-reversal mirror (TRM) [17]. General mathematical descriptions of its basic principle can be given as followings (For simplicity, we just use scalar fields here).

Assuming a short time domain pulse $p(t)$ emitted from a transmitter (acts as the source) which is located at $\boldsymbol{r}_s$, field propagates through the time-invariant heterogeneous media, illuminates a target situated at $\boldsymbol{r}'$. The incident field observed at $\boldsymbol{r}'$ due to the source is

$$u(\boldsymbol{r}', t) = p(t) * G_F(\boldsymbol{r}', \boldsymbol{r}_s, t) = \int p(\tau) G_F(\boldsymbol{r}', \boldsymbol{r}_s, t-\tau) d\tau, \quad (1)$$

where $G_F(\boldsymbol{r}', \boldsymbol{r}_s, t)$ is the Greens function, the symbol $*$ represents temporal convolution.

Then the target acts as a second source. The field is radiated back and received by an array of with K elements. The recorded signal on the kth element is

$$u_F(t, \boldsymbol{r}_k) \int \chi(\boldsymbol{r}') u(\boldsymbol{r}', t) * G_F(\boldsymbol{r}_k, \boldsymbol{r}', t) d\boldsymbol{r}'^2, \quad (2)$$

where $\chi(\boldsymbol{r}')$ is a characteristic function denotes the conversion of the incident field into equivalent scattered field $u(\boldsymbol{r}', t)$.

In the through wall application, the background information (like the dielectric constant and the approximate thickness of the wall) may be roughly estimated. The background signature can be measured as $u_{BF}(t, \boldsymbol{r}_k)$ a priori. Therefore, the target signature can be obtained by subtracting the background signature from the signature with the target in the background. So in the frequency domain, we have

$$U_{Fk}(\omega) = \int \left[\int \chi(\boldsymbol{r}') u(\boldsymbol{r}', t) * G_F(\boldsymbol{r}_k, \boldsymbol{r}', t) d\boldsymbol{r}'^2 - u_{BF}(t, \boldsymbol{r}_k) \right] \exp(-j\omega t) dt. \quad (3)$$

Signals are time reversed and re-emitted from the respective positions. The space-time signal observed at the imaging domain is

$$I(\boldsymbol{r}, t) = \sum_{k=1}^{K} \int [U_{Fk}(\omega)]^* G_C(\boldsymbol{r}, \boldsymbol{r}_k) \exp(j\omega t) d\omega, \quad (4)$$

where $G_C(\boldsymbol{r}, \boldsymbol{r}_k)$ represents the computational Green's function from the kth receiver (element) to the imaging domain (The symbol "$*$" denotes complex conjugation).

Usually, according to the imaging principle, the focusing quality (resolution) is determined by the size of the receiver array aperture.

In a heterogeneous, multipath environment, TRM technique can achieve much better resolution [18, 33]. This phenomenon is called super-resolution and comes from multipath caused by the media heterogeneities. TRM technique is widely regarded as a powerful method to image and detect targets in the complex environments. For the sake of saving space, more detailed knowledge about TRM is not mentioned here, the interested reader may consult the References [18, 34–42]. [18] presented the physical experiments, [35, 36] gave the mathematical analyzes in one-dimensional and layered media and [34] for three dimensional acoustic and electromagnetic waves in random media. [37, 38] show the self-averaging and statistical stability properties of time reversal. [39–42] reported some new applications of TRM (such as application in the Microwave-Induced Thermo-Acoustic Tomography (MI-TAT) for early breast cancer detection).

3. TRM TECHNIQUE IN TWR IMAGING

Some electromagnetic requirements for UWB TWR have been investigated in [4, 5]. A practical operational frequency is suggested about 1–3 GHz. Experimental measurements show that the complex TWR environment can result in considerable attenuation of electromagnetic waves, further more cause a complicated processing of received signals because of the multipath propagations. Considering the complex feature of TWR and the powerful use of TRM in the complex and high noise environment, we are particularly interested in simulating the TRM technique in TWR imaging. The FDTD algorithm is employed here for the simulation. We have performed a number of tests with numerical data to validate the 2-D electromagnetic time reversal imaging in the through wall environment.

In the following, we give a main description of the simulation settings in the Part 3.1. Then detailedly investigate the TRM technique to image targets behind a single- and multi-layered wall in Parts 3.2 and 3.3, respectively. The imaging results of TRM are compared with that of using the back projection imaging algorithm for a contrast of the imaging quality. Finally, we investigate the TRM imaging for the case in which there is a mismatch between the walls associated with the forward and inverse phases of time reversal in Part 3.4 for examining the stability of the method.

3.1. Description of the Model

As UWB radar has much wider bandwidth than convention narrow-band radar, it is believed to have great potential in high resolution

imaging. Here we assume the TWR uses UWB system. The UWB electromagnetic source is chosen as [43]

$$S(t) = \frac{j}{[j + 2\pi f(t - t_0)/4]^5} \tag{5}$$

with a center frequency $f = 2\,\text{GHz}$. j is the imaginary unit. The 3 dB frequency band is from 1.4 to 3.0 GHz. The electric fields are polarized vertically to the z direction.

In the simulation, we refer to the following two settings (the geometries are depicted in Fig. 2). Setting 1: The imaging domain is a 100 cm × 100 cm square region with its center at the origin point (i.e., the imaging domain is $[-50, 50] \times [-50, 50]$). A linear array of 19 receivers with an interval of 6 cm is located symmetrically along the line $x = -77\,\text{cm}$ with the 10th receiver (i.e., the center one) positioned at $y = 0$. A wall of 9 cm thickness and of 120 cm in the vertical direction is set parallel to the array with its center at $(-54.5, 0)$. The source is positioned at $(-67.5, 0)$. Some disc scatters behaving as targets will be settled in the imaging domain. The disc scatters used in the simulation are of the same media parameters $(\varepsilon_r, \mu_r) = (47, 0.21)$ and the same radius of 6 cm. Their positions will be given in every experiment. In the FDTD algorithm, the simulation domain is discretized to a number of cells with the size of 0.3 cm × 0.3 cm, equals to about 50 cells per wavelength in free space at the center frequency of 2 GHz.

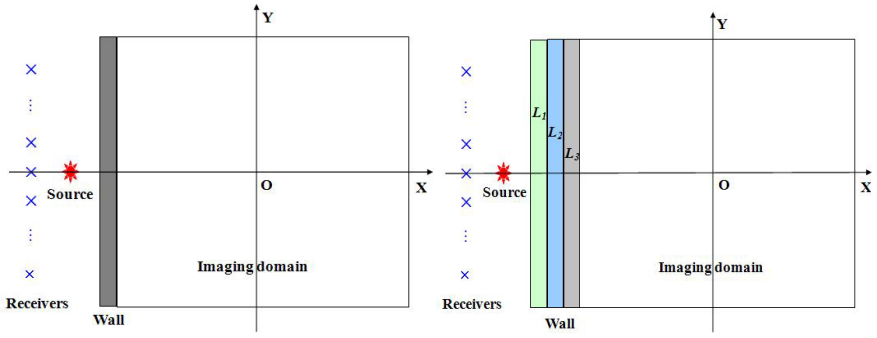

Figure 2. The sketch map of simulation settings. Setting 1 (left) is the single-layered wall environment. The media parameters are: $(\varepsilon_r, \mu_r) = (4, 0.002)$. Setting 2 (right) is the Multi-layered wall environment. The media parameters (ε_r, μ_r) of the layers are: L_1 (4.0, 0.002), L_2 (4.5, 0.0022) and L_3 (5.0, 0.0025). Compared with Setting 1, the difference is 18 cm left shift of the array and the source in the x-axis.

Setting 2 is similar to Setting 1. The difference is the multi-layered wall. Three layers are set adjacently with the same thickness of 9 cm but different media parameters as depicted in the Fig. 2. Corresponding modifications are stated in the figure's caption.

3.2. Single-layered Wall Imaging

For the Setting 1, we firstly consider a disc scatter situated at the origin point. The target signal from the 10th receiver is shown in Fig. 3. The amplitude attenuation of the target signal is about -50 dB. As to show the temporal refocusing, in Fig. 4, we plot the maximum amplitudes of the imaging domain along the time axis. From the figure, we can see that a temporal refocusing is gained at the time $t_c = 5.80$ ns. Here $t = 0$ represents the time when signals were re-emitted from the array of receivers (the same hereinafter).

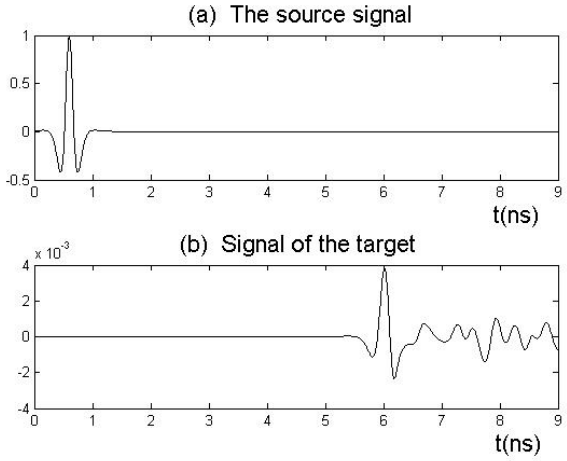

Figure 3. (a) is the source signal used in the simulation. (b) is the signal of the target from the 10th receiver.

Figure 5 gives the spatial refocusing at time t_c. We can see that the target position in the figure agrees very well with the experimental setting which means a tight spatial focusing at the target's location. The discussion above implies a good strategy to determine the temporal refocusing and give an exact spatial refocusing. This imaging strategy will be used in the following time reversal imaging experiments.

In the Fig. 6, the back projection method imaging result of the received signal is given as a comparison. It is clear that the focusing

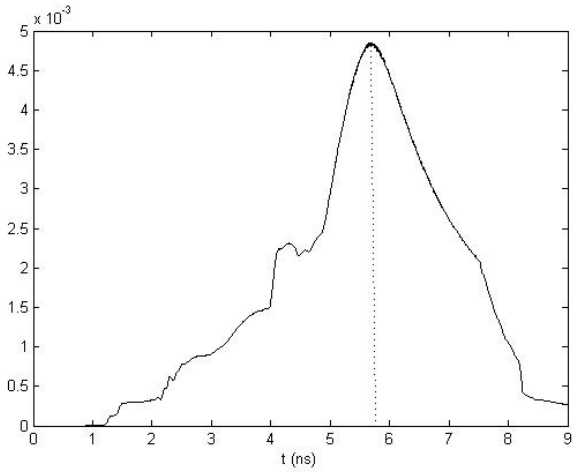

Figure 4. The maximum amplitude line of the imaging domain along the time axis.

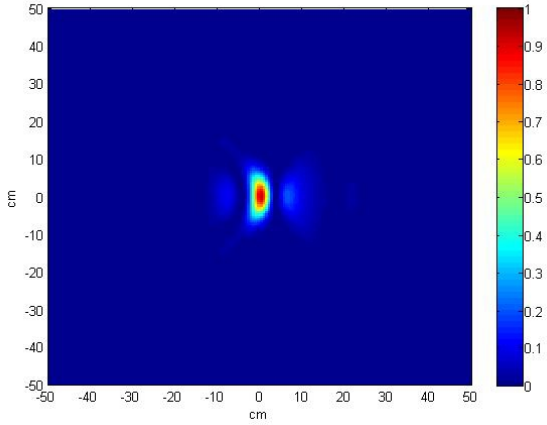

Figure 5. In the single-layered wall environment, the TRM imaging of the disc scatter which is settled at the center of the imaging domain.

of TRM is much better than that of the back projection method. The TRM imaging bears twice Signal-to-Noise Ratio (SNR) as compared with the back projection imaging. And it is noticed that position of the target in Fig. 6 is a little bit back of the real position. This is because the received signal is delayed in the propagation caused by the wall but the back projection imaging can not put this delay into

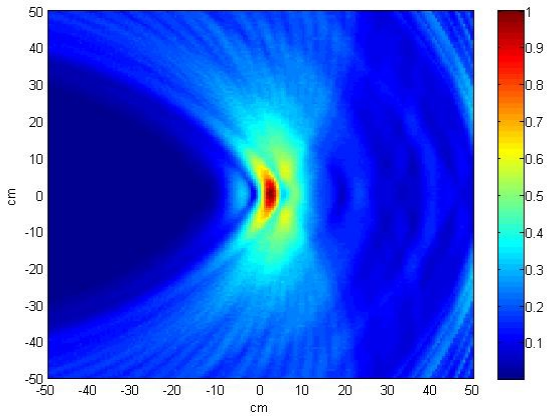

Figure 6. The back projection imaging result. The setting is the same as that described in Fig. 5's caption.

account.

Secondly, two disc scatters are settled symmetrically at the points (0, 20) and (0, −20). Because of their absolute symmetry, they will have the same temporal refocusing. Following the imaging strategy mentioned above, we show in Fig. 7 the tight spatial focusing from TRM. For the contrast, the imaging from the back projection method is given in Fig. 8. Clearly, the TRM imaging can well separate the two targets and give their exact refocusing positions. The SNR of TRM imaging is nearly 2.6 times as the back projection imaging under this condition. In Fig. 8, there is a distinct coupling between the two targets induced by target inter-scattering which implies a worse resolution than Fig. 7.

For further simulation, two disc scatters are put non-symmetry in the imaging domain. They are positioned at (−25, −25) and (7, 20), respectively. Because the distances from the original transmitter to the two targets are different, the currents induced by the incident field on the two targets are different. The two scatters act as two different second sources. Even TRM is used, the EM signals would be refocused at different times. Considering the process of iteratively radiating mentioned in [17], we place a null in the direction of the dominant scattering center. After successive iterations, space-time energy localization now occurs at the second strongest scattering center. When there is more than one target in the imaging domain, this procedure can be repeated to image the scattering targets, from the strongest to the weakest. Figs. 9(a) and (b) are the TRM imaging

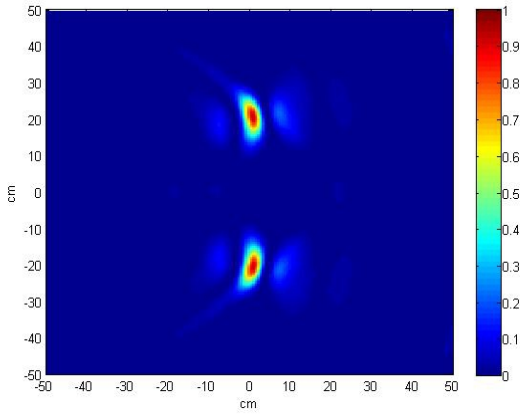

Figure 7. In the single-layered wall environment, the TRM imaging of the two disc scatters which are settled symmetrically at the points (0, 20) and (0, −20).

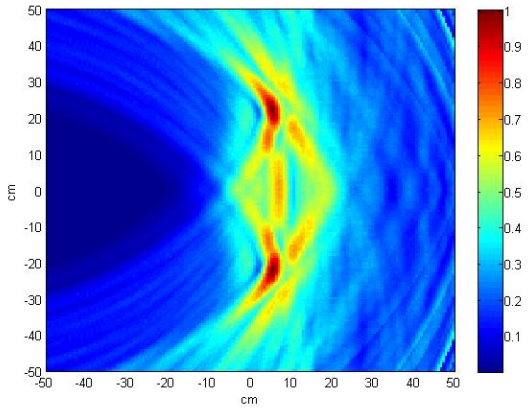

Figure 8. In the single-layered wall environment, the back projection imaging of the two disc scatters which are settled symmetrically at the points (0, 20) and (0, −20).

results for the two targets. For contrast, the back projection imaging is given in Fig. 10. When there is more than one target arbitrarily displayed in the imaging domain, the back projection method can't image all the targets exactly under current setting. There is about 25 cm right translation of the later target in the figure. This is because the two targets behaved as two second sources but don't reflect the waves at the same time.

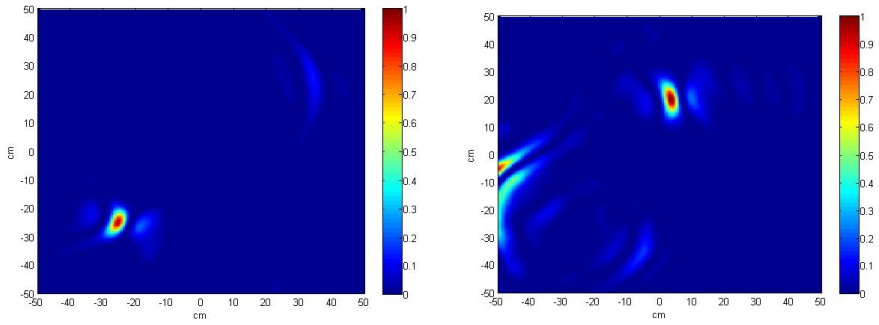

(a) (b)

Figure 9. TRM imaging of the two disc scatters which are positioned at $(-25, -25)$ and $(7, 20)$, respectively. (a) is the image of the former one and (b) is the later one.

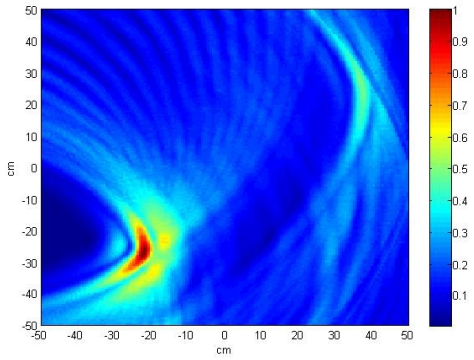

Figure 10. The back projection imaging of the two disc scatters which are positioned at $(-25, -25)$ and $(7, 20)$, respectively.

3.3. Multi-layered Wall Imaging

In this sub section, we consider a more complex setting (as shown in Fig. 2). Assuming the wall is composed of three layers with different media parameters. We investigated the single target imaging firstly. The target is situated at the origin point. Fig. 11 shows the imaging result from TRM. Tight spatial focusing is also observed at the target's location. Compared with Fig. 5, the TRM imaging here keeps nearly the same SNR (21 dB) and resolution. Fig. 12 is the imaging result from back projection method. Because of the distortion and delay of the multi-layered wall, a more visible deviation of the target position

in the horizontal direction and a decent of resolution in the vertical direction can be seen compared with Fig. 6. Fig. 13 is the TRM imaging result when the two targets are centered symmetrically at the point (0, 20) and (0, −20). Fig. 14 shows the corresponding imaging result from the back projection method.

For the multi-layered wall case, the complex environment is employed by TRM but behaves as a holdback when we apply the back projection method. As a result, the tight refocusing, as well as in the

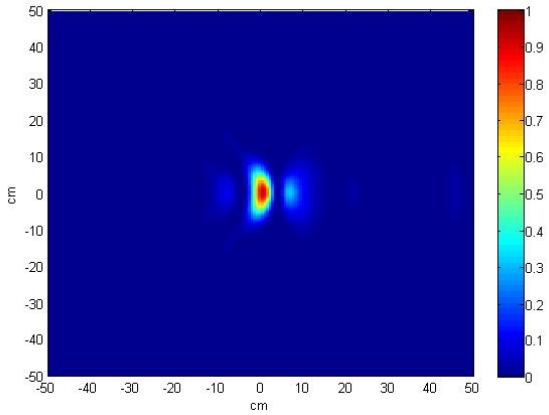

Figure 11. In the multi-layered wall environment, the TRM imaging of the disc scatter which is settled at the center of the imaging domain.

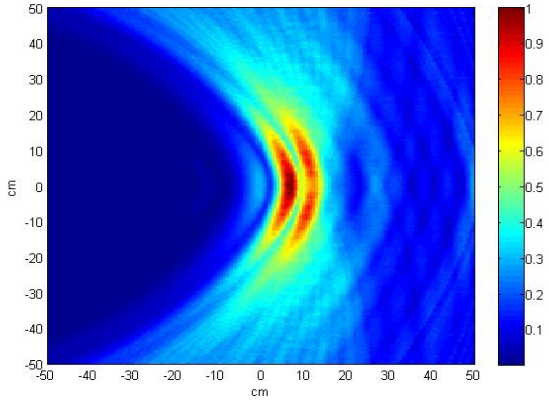

Figure 12. In the multi-layered wall environment, the back projection imaging of the disc scatter which is settled at the center of the imaging domain.

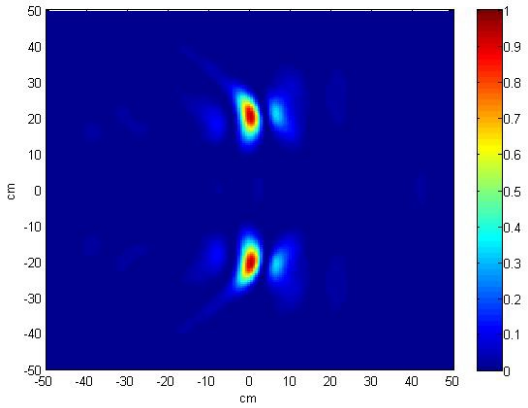

Figure 13. In the multi-layered wall environment, the TRM imaging of the two disc scatters which are settled symmetrically at the points (0, 20) and (0, −20).

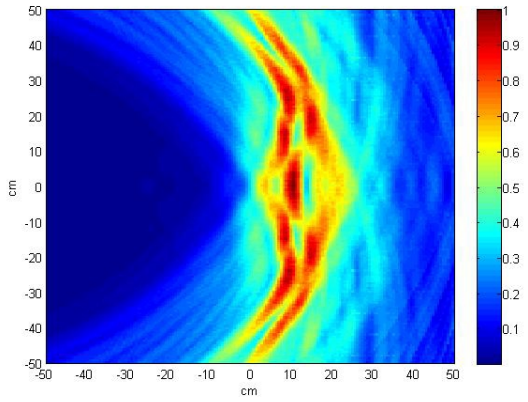

Figure 14. In the multi-layered wall environment, the back projection imaging of the two disc scatters which are settled symmetrically at the points (0, 20) and (0, −20).

single-layered wall case is obtained through TRM while de-focusing and de-resolution are shown by using the back projection method.

3.4. TRM Imaging in Changing Media

An important issue of interest concerns time reversal image stability. Theoretical studies [32] illuminate that the refocusing quality of the back-propagated signals is determined by the cross-correlation of the

two media. When the two media deteriorate, de-refocusing effects are observed. Under some wave propagation mode (for instance, in the paraxial regime), refocusing in the high frequency is statistically stable, that is, independent of the realizations of the two media. Experimental studies of electromagnetic TRM [28] demonstrated a fair refocusing at the targets location in spite of media interchanging and a substantial deterioration of the TRM image as the media de-correlation increases.

To examine this issue in the TWR imaging, one disc scatter is settled in the center of the imaging domain in Setting 2. Different walls are realized by interchanging the orders of the three layers in Fig. 2. In the forward propagation phase, the order of the three layers is fixed as $L_1L_2L_3$, as shown in Fig. 2. When the time reversed field re-emitted into the space, the layers' orders are interchanged as $L_2L_3L_1$ and $L_3L_2L_1$, respectively. We investigate how the imaging changes if the time reversed field propagates through the two different walls. Figs. 15(a) and (b) show the imaging results. It is clear that the observations are consistent with previous studies in [28, 32]. A fair refocusing is observed at the target's location. The SNR here are lower than Fig. 11 (the SNR for (a) and (b) are 15.6 dB and 16.2 dB, respectively). The observation also shows a reduction of the resolution when compared with Fig. 11.

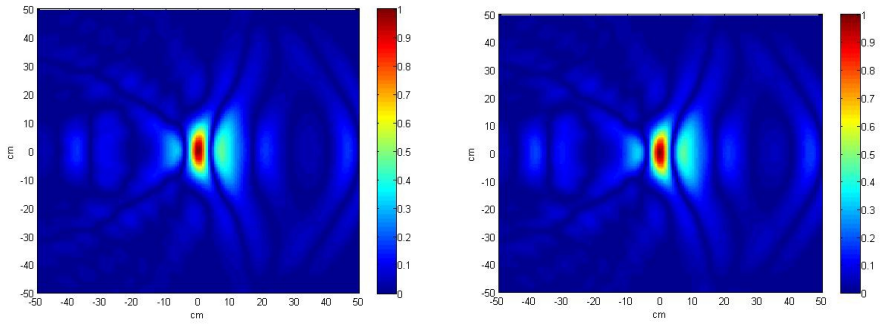

(a) (b)

Figure 15. TRM imaging for the case in which there is mismatch between the media associated with the forward and inverse phases of TRM method. (a) and (b) are the target images from the case of $L_2L_3L_1$ and $L_3L_2L_1$, respectively.

4. CONCLUSIONS

TRM imaging technique has been examined through simulation experiment for electromagnetic wave in the through wall environment in this communication. We investigated the well-known time reversal behavior for the single- and multi-layered wall environments to image one and two scatters. Compared with back projection method, higher imaging quality is obtained. After the study of TRM in the matched media, TRM is demonstrated in the changing media. Observations show a reduction of the resolution and SNR but a fair refocusing at the target's location.

Main work of this communication is introducing the TRM technique to TWR imaging and giving some preliminary results based on the numerical simulation. For the real applications, more complex environments concern wall of rough surface and random media should be taken into account. The further work is being undertaken.

ACKNOWLEDGMENT

This work is supported in part by the NSFC (No. 60771042), 863 Program (No. 2007AA12Z159), Program for New Century Excellent Talents in University of China and 08ZQ026-039 sustentation fund.

REFERENCES

1. Ferris, Jr., D. D. and N. C. Currie, "A survey of current technologies for through-the-wall surveillance," *Proc. SPIE*, Vol. 3577, 62–72, 1998.
2. Hunt, A. R., "A wideband imaging radar for through-the-wall surveillance," *Proc. SPIE*, Vol. 5403, 590–596, 2004.
3. Borek, S. E., "An overview of through the wall surveillance for homeland security," *IEEE, Proceedings of the 34th Applied Imagery and Pattern Recognition Workshop*, 6–11, 2005.
4. Zhuge, X., T. G. Savalyev, and A. G. Yarovoy, "Assessment of electromagnetic requirements for UWB through-wall radar," *IEEE, Proc. ICEAA*, 923–926, 2007.
5. Yang, Y. and A. E. Fathy, "See-through-wall imaging using ultra wideband short-pulse radar system," *IEEE, Anten. and Propag. Society International Symposium*, Vol. 38, 334–337, 2005.
6. Yang, Y., Y. Wang, and A. E. Fathy, "Design of compact Vivaldi antenna arrays for UWB see through wall applications," *Progress In Electromagnetics Research*, PIER 82, 401–418, 2008.

7. Hunt, A. R., "A wideband imaging radar for through-the-wall surveillance," *Proc. SPIE*, Vol. 5403, 590–596, 2004.
8. Beeri, A. and R. Daisy, "High-resolution through wall imaging," *Proc. SPIE*, Vol. 6201, 62010J, 2006.
9. Hunt, A. R., "Image formation through walls using a distributed radar sensor array," *Applied Imagery Pattern Recognition Workshop*, 232–237, 2003.
10. Fan, Z. G., L. X. Ran, and J. A. Kong, "Source pulse optimizations for UWB radio systems," *Journal of Electromagnetic Waves and Applications*, Vol. 20, 1535–1550, 2006.
11. Zetik, R., S. Crabbe, J. Krajnak, P. Peyerl, J. Sachs, and R. Thoma, "Detection and localization of persons behind obstacles using Msequence through-the-wall radar," *Proc. SPIE*, Vol. 6201, 62010I, 2006.
12. Song, L.-P., C. Yu, and Q. H. Liu, "Through-wall imaging (TWI) by radar: 2-D tomographic results and analyses," *IEEE Transactions on Geoscience and Remote Sensing*, Vol. 43, 2793–2798, 2005.
13. Cui, G., L. Kong, and J. Yang, "A back-projection algorithm to stepped-frequency synthetic aperture through-the-wall radar imaging," *Process of 1st Asian and Pacific Conference on Synthetic Aperture Radar*, 123–126, 2007.
14. Abubakar, A., P. M. van den Berg, and S. Y. Semenov, "Two and three dimensional algorithms for microwave imaging and inverse scattering," *Progress In Electromagnetics Research*, PIER 37, 57–79, 2002.
15. Song, L. P., Q. H. Liu, F. Li, and Z. Q. Zhang, "Reconstruction of three dimensional objects in layered media: Numerical experiments," *IEEE Trans. Antennas Propagat.*, Vol. 53, 1556–1561, 2005.
16. Ahmad, F., M. G. Amin, and G. Mandapati, "Autofocusing of through-the-wall radar imagery under unknown wall characteristics," *IEEE Transactions on Image Processing*, Vol. 16, 1785–1795, 2007.
17. Fink, M., "Time reversal of ultrasonic fields-part I: Basic principles," *IEEE Transactions on Ultrasonics, Ferroelectrics, and Frequency Control*, Vol. 39, 555–566, 1992.
18. Fink, M., "Time reversed acoustics," *Physics Today*, Vol. 50, 34–40, 1997.
19. Derode, A., P. Roux, and M. Fink, "Robust acoustic time reversal with high-order multiple scattering," *Phys. Rev. Lett.*, Vol. 75,

4206–4209, 1995.

20. Kim, S., G. F. Edelmann, W. A. Kuperman, W. S. Hodgkiss, H. C. Song, and T. Akal, "Spatial resolution of time-reversal arrays in shallow water," *J. Acoust. Soc. Am.*, Vol. 110, 820–829, 2001.
21. Borcea, L., C. Tsogka, G. Papanicolaou, and J. Berryman, "Imaging and time reversal in random media," *Inverse Problems*, Vol. 18, 1247–1279, 2002.
22. Tsogka, C. and G. Papanicolaou, "Time reversal through a solid-liquid interface and super-resolution," *Inverse Problems*, Vol. 18, 1639–1657, 2002.
23. Papanicolaou, G., L. Ryzhik, and K. Solna, "The parabolic wave approximation and time reversal," *Matematica Contemporanea*, Vol. 23, 139–160, 2002.
24. Lerosey, G., J. de Rosny, A. Tourin, A. Derode, G. Montaldo, and M. Fink, "Time reversal of electromagnetic waves," *Phys. Rev. Lett.*, Vol. 92, 1939041-3, 2004.
25. Liu, D., G. Kang, L. Li, Y. Chen, S. Vasudevan, W. Joines, Q. H. Liu, J. Krolik, and L. Carin, "Electromagnetic time-reversal imaging of a target in a cluttered environment," *IEEE Trans. Antennas Propagat.*, Vol. 53, 3058–3066, 2005.
26. Tortel, H., G. Micolau, and M. Saillard, "Decomposition of the time reversal operator for electromagnetic scattering," *Journal of Electromagnetic Waves and Applications*, Vol. 13, 687–719, 1999.
27. Liu, D., J. Krolik, and L. Carin, "Electromagnetic target detection in uncertain media: Time-reversal and minimum-variance algorithms," *IEEE Transactions on Geoscience and Remote Sensing*, Vol. 45, 934–944, 2007.
28. Liu, D., S. Vasudevan, J. Krolik, G. Bal, and L. Carin, "Electromagnetic time-reversal source localization in changing media: Experiment and analysis," *IEEE Trans. Antennas Propagat.*, Vol. 55, 344–354, 2007.
29. Chen, X., "Time-reversal operator for a small sphere in electromagnetic fields," *Journal of Electromagnetic Waves and Applications*, Vol. 21, 1219–1230, 2007.
30. Rao, T. and X. Chen, "Analysis of the time-reversal operator for a single cylinder under two-dimensional settings," *Journal of Electromagnetic Waves and Applications*, Vol. 20, 2153–2165, 2006.
31. Chambers, D. H. and J. G. Berryman, "Analysis of the time-reversal operator for a small spherical scatterer in an

electromagnetic field," *IEEE Trans. Antennas Propag.*, Vol. 52, 1729–1738, 2004.

32. Bal, G. and R. Verastegui, "Time reversal in changing environment," *SIAM Mult. Mod. Simul.*, Vol. 2, 639–661, 2004.
33. Blomgren, P., G. Papanicolaou, and H. Zhao, "Super-resolution in time-reversal acoustics," *J. Acoust. Soc. Am.*, Vol. 111, 230–248, 2002.
34. Bal, G. and L. Ryzhik, "Time reversal and refocusing in random media," *SIAM J. Appl. Math*, Vol. 63, 1475–1498, 2003.
35. Clouet, J. F. and J. -P. Fouque, "A time-reversal method for an acoustical pulse propagating in randomly layered media," *Wave Motion.*, Vol. 25, 361–368, 1997.
36. Fouque, J.-P. and K. Sqlna, "Time reversal aperture enhancement," *SIAM Mult. Mod. Simul.*, Vol. 1, 239–259, 2003.
37. Bal, G., G. Papanicolaou, and L. Ryzhik, "Self-averaging in time reversal for the parabolic wave equation," *Stochastics and Dynamics*, Vol. 2, 507–531, 2002.
38. Papanicolaou, G., L. Ryzhik, and K. Solna, "Statistical stability in time reversal," *SIAM J. on Appl. Math.*, Vol. 64, 1133–1155, 2004.
39. Chen, G. P., W. B. Yu, Z. Q. Zhao, et al., "The prototype of microwave-induced thermo-acoustic tomography imaging by time reversal mirror," To appear in *Journal of Electromagnetic Waves and Applications*, 2008.
40. Chen, G. P., Z. Q. Zhao, and Q. H. Liu, "Computational study of time reversal mirror technique for microwave-induced thermo-acoustic tomography," *Journal of Electromagnetic Waves and Applications*, Vol. 22, 2191–2204, 2008.
41. Xiao, S. Q., J. Chen, B.-Z. Wang, and X. F. Liu, "A numerical study on time-reversal electromagnetic wave for indoor ultra-wideband signal transmission," *Progress In Electromagnetics Research*, PIER 77, 329–342, 2007.
42. Liu, X., B.-Z. Wang, S. Xiao, and J. Deng, "Performance of impulse radio UWB communications based on time reversal technique," *Progress In Electromagnetics Research*, PIER 79, 401–413, 2008.
43. Zhao, Z., N. Li, J. Smith, and L. Carin, "Analysis of scattering from very large three-dimensional rough surface using MLFMM and ray-based analyses," *IEEE Antennas and Propagation Magazine*, Vol. 47, 20–30, 2005.